

## PHAGOCYTES, GRANULOCYTES, AND MYELOPOIESIS

## RhoA determines disease progression by controlling neutrophil motility and restricting hyperresponsiveness

Richard T. Jennings,<sup>1</sup> Monika Strengert,<sup>1</sup> Patti Hayes,<sup>1</sup> Jamel El-Benna,<sup>2</sup> Cord Brakebusch,<sup>3</sup> Malgorzata Kubica,<sup>1</sup> and Ulla G. Knaus<sup>1</sup>

<sup>1</sup>Conway Institute, School of Medicine and Medical Science, University College Dublin, Dublin, United Kingdom; <sup>2</sup>INSERM U773, Université Paris 7 Denis Diderot, Sorbonne Paris Cité, Laboratoire d'Excellence Inflammex, Paris, France; and <sup>3</sup>Biomedical Institute, Biotech Research and Innovation Centre, University of Copenhagen, Copenhagen, Denmark

## Key Points

- Rho-deficient neutrophils are hyperresponsive.
- RhoA acts predominantly as a negative regulator of chemotaxis.

**Neutrophil responses are central to host protection and inflammation. Neutrophil activation follows a 2-step process in which priming amplifies responses to activating stimuli. Priming is essential for life span extension, chemotaxis, and respiratory burst activity. Here we show that the cytoskeletal organizer RhoA suppresses neutrophil priming via formins. Premature granule exocytosis in Rho-deficient neutrophils activated numerous signaling pathways and amplified superoxide generation. Deletion of Rho altered front-to-back coordination by simultaneously increasing uropod elongation, leading edge formation, and random migration. Concomitant negative and positive regulation of  $\beta_2$  integrin-independent and  $\beta_2$  integrin-dependent migration, respectively, reveal Rho as a key decision point in the neutrophil response to discrete chemotactic agents. Although even restricted influx of Rho-deficient hyperactive neutrophils exacerbated lipopolysaccharide-mediated lung injury, deleting Rho in innate immune cells was highly protective in influenza A virus infection. Hence, Rho is a key regulator of disease progression by maintaining neutrophil quiescence and suppressing hyperresponsiveness. (*Blood*. 2014;123(23):3635-3645)**

## Introduction

Beyond their essential role in acute infections and in modulating the adaptive immune response, neutrophils promote severe inflammation and tissue damage in acute and chronic inflammatory diseases.<sup>1,2</sup> For example, neutrophils are recognized as the key cell type in the pathogenesis of acute lung injury (ALI) triggered by bacterial products, chemicals, hyperoxia, high pressure ventilation, or reperfusion, but at the same time their antimicrobial activity is crucial for host defense. Thus fine-tuning neutrophil responses has attracted considerable interest. When recruited to sites of infection or injury, neutrophils undergo discrete changes, termed *priming responses*, which can be induced by cytokines, lipopolysaccharide (LPS), leukotriene B<sub>4</sub>, and adhesion to extracellular matrix. Only upon encountering “end-target” signals such as pathogen-derived peptides (fMLF) or complement fragments (C5a) will the fully active state be attained.<sup>3</sup> The priming phase is characterized by exocytosis of several granule subsets, thereby increasing surface expression and activity of adhesion molecules, receptors, and nicotinamide adenine dinucleotide phosphate (NADPH) oxidase (Nox2-p22<sup>phox</sup>). Priming is accompanied by distinct phosphorylations and partial oxidase assembly, representing the so-called “ready to go” state, that by itself cannot generate reactive oxygen species (ROS) but markedly augments ROS production upon full neutrophil activation.<sup>4</sup> Activated neutrophils also release antimicrobial peptides, myeloperoxidase, cytokines, proteases, and extracellular traps (NETs), thus promoting pathogen destruction as well as vascular permeability and endothelial damage.

Rho family GTPases are key regulators of cytoskeletal organization required for specialized neutrophil functions including adhesion, cell polarization, directional migration, phagocytosis, and microbial killing.<sup>5</sup> Gene-targeting studies using myeloid lineage-specific drivers showed that Rac1, Rac2, and Cdc42 are involved in various steps of polarization, integrin-mediated spreading, actin polymerization, chemotaxis, and phagocytosis.<sup>6,7</sup> Rac1, Rac2, or Cdc42 deficiency in innate immune cells attenuated migration *in vivo*.<sup>6,8</sup> Moreover, Rac2 is essential for primary granule release and NADPH oxidase activation, both prerequisites for microbial killing.<sup>9</sup>

The contribution of RhoA, the main Rho isoform in neutrophils, can only be deduced from cell line-based studies, because RhoA deletion is lethal in early embryogenesis. RhoA regulates actin dynamics and contractility through the downstream targets ROCK1/2 and mDia1-3 formins.<sup>10</sup> ROCK phosphorylates LIM kinase, MLC phosphatase, and myosin light chain, leading to stabilization of actin filaments and formation of actomyosin bundles, whereas mDia catalyzes actin polymerization and stabilization of microtubules. RhoA knockdown in T cells or PLB-985 cells inhibits both SDF-1 $\alpha$ -mediated transendothelial migration and fMLF-induced chemotaxis.<sup>11,12</sup> Further, RhoA-mDia signaling has been implicated in CR3- and Fc $\gamma$ -mediated phagocytosis.<sup>13-15</sup>

Although the Rho-ROCK pathway is considered a promising target for therapeutic intervention in inflammatory disease, our understanding of Rho proteins as regulators of neutrophil functions

Submitted February 22, 2014; accepted April 18, 2014. Prepublished online as *Blood* First Edition paper, April 29, 2014; DOI 10.1182/blood-2014-02-557843.

The publication costs of this article were defrayed in part by page charge payment. Therefore, and solely to indicate this fact, this article is hereby marked “advertisement” in accordance with 18 USC section 1734.

The online version of this article contains a data supplement.

© 2014 by The American Society of Hematology

remains limited.<sup>7,10</sup> To better understand how disruption of Rho signaling will alter neutrophil biology, mice with myeloid lineage-specific RhoA and combined RhoA/RhoB deletion were generated. We show here that RhoA acts as a rheostat suppressing premature neutrophil priming. Moreover, Rho discriminates between chemotactic stimuli, thus acting as a negative and positive regulator of neutrophil recruitment *in vitro* and *in vivo*. Rho deficiency in innate immune cells increased neutrophil flux toward  $\beta_2$  integrin-independent stimuli, but limited  $\beta_2$  integrin-dependent neutrophil recruitment. Even without efficient transmigration, Rho-deficient hyperactivated neutrophils exaggerated tissue injury in LPS-induced ALI. In contrast, an increased influx of hyperactivated neutrophils into the lung protected the host from lethal influenza A virus (IAV) challenge.

## Methods

### Mouse strains

RhoA<sup>loxp/loxp</sup>, LysM<sup>Cre/Cre</sup> and RhoB<sup>-/-</sup> strains have been reported<sup>16-18</sup> and were used to generate combination strains as indicated in Figure 1A. Age- (8-12 weeks) and gender-matched mice or gender-matched littermates were used. Survival experiments were terminated at a predetermined humane end point. Procedures were approved by the University College Dublin Institutional Animal Care and Use Committee and licensed by the Department of Health and Children.

### Neutrophil migration *in vitro*

Neutrophils were purified as described.<sup>19</sup> Neutrophils were placed on 3- $\mu$ m transwell filters coated with 12.5  $\mu$ g/mL bovine fibronectin for 30 minutes before 10  $\mu$ M fMLF or 200 ng/mL chemokine (C-X-C motif) ligand 1 (CXCL1) in Hank's Balance Salt Solution was added to the lower chamber. After 1 hour, images of the bottom wells were analyzed using ImageJ software. For certain studies, neutrophils were preincubated with 15  $\mu$ M Fasudil, 10  $\mu$ M LIMKi3, 10  $\mu$ M SMIFH2, 10  $\mu$ M Y-27632, 50 ng/mL Tat-C3, 2  $\mu$ M SB203580, 100 nM wortmannin, 5  $\mu$ M U0126, 10  $\mu$ g/mL superoxide dismutase (SOD), or 400 U/mL catalase. Three-dimensional migration through Nutragen was performed as described.<sup>20</sup> Random migration was recorded on fibronectin-coated glass dishes using an Andor (Olympus) Revolution Spinning disc microscope fitted heated chamber; UPLSAPO 60 $\times$ /1.35 (oil) objective for uropods and UPLSAPO 20 $\times$ /0.75 objective for random migration; camera iXonEM+897 EMCCD. Migration of 15 cells per movie was quantified in ImageJ using manual tracking and chemotaxis tools.

### Functional assays

GTPase activity and primary/secondary granule exocytosis were analyzed as reported.<sup>21,22</sup> Superoxide production was determined by luminol-enhanced chemiluminescence (suspension; in relative light units); H<sub>2</sub>O<sub>2</sub> generation by homovanillic acid assay (adherent; in relative fluorescent units).<sup>23</sup>

### Immunophenotyping

Neutrophils ( $1 \times 10^6$ ) were incubated with purified anti-mouse Fc $\gamma$ R (clone 2.4G2) to block binding of the labeled antibodies to Fc $\gamma$ R. After incubation for 30 minutes at 4°C, the cells were stained with predetermined optimal concentrations of the respective antibodies.

### *In vivo* peritonitis models

Mice were challenged via intraperitoneal (ip) injection with 2 mL phosphate-buffered saline 4% thioglycollate broth or 500  $\mu$ L PBS containing either 1 g/kg zymosan A or 10<sup>7</sup> *Escherichia coli* for 5 hours. Cells in the peritoneal lavage were analyzed by flow cytometry after phycoerythrin-conjugated anti-Ly6G staining.

### *In vivo* lung models

Mice were challenged via intranasal installation (in) with 30  $\mu$ g/kg CXCL1, 1 mg/kg fMLF, 1 mg/kg LPS, 10<sup>7</sup> *E coli*, or 10<sup>6</sup> pfu/kg IAV Hamburg/05/09 (pHH05)<sup>24</sup> in PBS. At indicated time points, bronchoalveolar lavage (BAL) was analyzed for cytokines using the multiplex-fluorokine assay (R&D Systems), for NET formation by Sytox Green (5  $\mu$ M) fluorometry, for type I IFNs, and for virus load as described.<sup>25-27</sup> Paraffin-embedded lung sections were stained with hematoxylin and eosin or modified Carstairs, and visualized with a Leica DFC300X camera and IM50 imaging software.

### Statistical analysis

Sample size (n) denotes biological replicates. Statistical analyses were performed as indicated in figure legends using GraphPad Prism, v5.

## Results

### RhoA deficiency triggers neutrophil priming

Mice with myeloid-specific RhoA deletion, RhoA<sup>loxp/loxp</sup>LysM<sup>Cre/Cre</sup> mice, were viable and healthy, but their neutrophils displayed highly increased RhoB levels. To alleviate potential compensation, RhoA<sup>loxp/loxp</sup>LysM<sup>Cre/Cre</sup> mice were crossed with RhoB<sup>-/-</sup> mice<sup>18</sup> to obtain mice with complete Rho deficiency in the myeloid compartment (RhoA/B dKO), because RhoC protein was not detected (Figure 1A-B). Initially RhoA KO, RhoB KO, and RhoA/B dKO neutrophils and their respective controls were compared, but RhoB-deficient neutrophils resembled wild-type (WT) neutrophils so closely that RhoB KO<sup>2</sup> littermates of RhoA/B dKO mice were used as controls when appropriate.

Neutrophils derived from RhoB KO<sup>2</sup> or RhoA/B dKO mice were probed for expression and steady-state activation of Cdc42 and Rac, because regulation of related Rho GTPases is often interconnected. No changes in Rac and Cdc42 activity or expression were detected (Figure 1C). Rho signaling to effectors such as mDia1 promotes actin nucleation and filament assembly. Comparison of F-actin generation in RhoB KO<sup>2</sup> vs RhoA/B dKO neutrophils revealed reduced F-actin levels at baseline and upon fMLF or CXCL1 stimulation (Figure 1D). F-actin distribution was also altered at baseline by redistributing actin to the periphery instead of localization throughout the cell (Figure 1E, quantification supplemental Figure 1A-C available on the *Blood* Web site). Both RhoB KO and RhoA/B dKO neutrophils displayed F-actin accumulation at the leading edge and polarization into one dominant pseudopod upon stimulation with either fMLF or CXCL1. Thus RhoA/B dKO neutrophils are capable of polarizing but displayed this phenotype before stimulation (quantification supplemental Figure 1D).

Actin filaments dispersed throughout quiescent neutrophils may restrict access of granules to the plasma membrane. Because the cytoskeleton has been implicated in degranulation,<sup>28</sup> the release of myeloperoxidase (MPO) from primary granules and of lactoferrin from secondary granules was determined. Although MPO secretion was not affected by the absence of Rho (supplemental Figure 1E), basal and stimulus-mediated lactoferrin secretion was significantly enhanced (Figure 1F). In addition, p38 MAPK activity has been linked with granule exocytosis.<sup>29</sup> Analysis of p38 phosphorylation revealed substantial upregulation of basal p38 activity in RhoA/B dKO neutrophils (Figure 1G). Further, CD62L shedding, indicating neutrophil activation, and the mobilization of secondary granule proteins including the antimicrobial peptide CRAMP or formylpeptide receptor (FPR) to the cell surface were assessed. In quiescent conditions, both CRAMP and FPR cell surface expression was upregulated in RhoA/B dKO neutrophils, whereas a fraction of

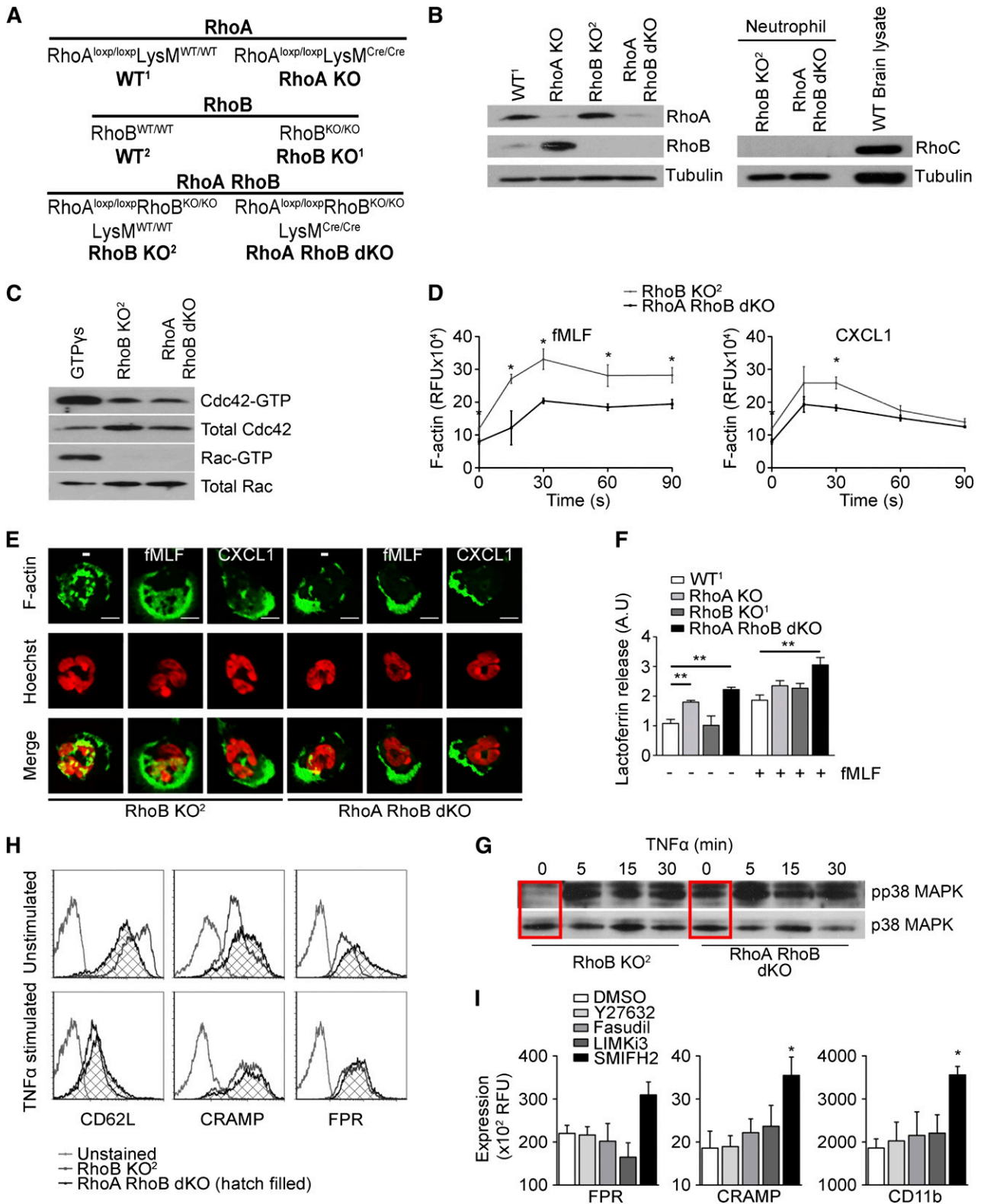


**Figure 1. Neutrophils deficient in RhoA and RhoB are preactivated.** (A) Genotypes and designations of mouse strains used in this study. (B) Immunoblots (IB) depicting RhoA, RhoB, and RhoC expression in neutrophils derived from the indicated mouse strains. Tubulin served as loading control and mouse brain lysate as RhoC control. (C) Cdc42 and Rac1 activity in unstimulated, Rho-deficient neutrophils in suspension. (D) Analysis of F-actin content of RhoB KO<sup>2</sup> and RhoA/B dKO neutrophils upon stimulation with fMLF and CXCL1. (E) F-actin distribution in RhoB KO<sup>2</sup> and RhoA/B dKO neutrophils stimulated with vehicle, fMLF, or CXCL1. The scale bar represents 5 μm. (F) Analysis of secondary granule exocytosis of RhoA KO, RhoB KO<sup>1</sup>, and RhoA/B dKO neutrophils after treatment as indicated, displayed as lactoferrin release relative to unstimulated WT<sup>1</sup> neutrophils. (G) Phosphorylation of p38 MAPK in suspension neutrophils as indicated, stimulated with 10 ng/mL TNFα as indicated; total p38 served as control. (H-I) Surface expression of CD62L, CRAMP, and FPR on RhoB KO<sup>2</sup> and RhoA/B dKO neutrophils (H) or WT<sup>1</sup> neutrophils pretreated with inhibitors. Means ± SEM (n = 3): (D) \*P < .05, \*\*P < .01, unpaired 2-tailed Student t test; (F) \*P < .05, \*\*P < .01 by 2-way analysis of variance (ANOVA) post-hoc Bonferroni multiple comparison; (I) \*P < .05, \*\*P < .01 by 1-way ANOVA post-hoc Dunnett's multiple comparison.

CD62L was prematurely shed, indicating a stimulus-independent, primed phenotype (Figure 1H). After tumor necrosis factor- $\alpha$  (TNF $\alpha$ ) priming, RhoB KO and RhoA/B dKO neutrophil cell surface expression of these markers was comparable. Treatment of WT neutrophils with several inhibitors of Rho effectors such as ROCK, LIM kinase, or formins, revealed that only SMIFH2, an inhibitor of mDia, augmented granule exocytosis (Figure 1I), suggesting that RhoA signaling controls neutrophil degranulation via formin-mediated actin filament assembly.

### RhoA regulates the amplitude of receptor-mediated ROS generation

Neutrophil priming is crucial for amplification of the NADPH oxidase-mediated respiratory burst. Premature mobilization of FPR and the Nox2-p22<sup>phox</sup> complex will likely lead to increased ROS generation. In neutrophils derived from WT<sup>1</sup>, WT<sup>2</sup>, RhoB KO<sup>1</sup>, and RhoB KO<sup>2</sup> mice, prior TNF $\alpha$  priming was required for fMLF-mediated superoxide generation, whereas TNF $\alpha$  or fMLF treatment alone did not trigger significant ROS production (Figure 2A). In contrast, unprimed RhoA KO neutrophils generated superoxide upon fMLF stimulation, which was further amplified by prior TNF $\alpha$  exposure (Figure 2A, first panel). This preactivated phenotype was further enhanced in neutrophils lacking both Rho isoforms. Superoxide levels generated by fMLF-stimulated, unprimed RhoA/B dKO neutrophils were comparable with fully activated neutrophils derived from WT or RhoB KO mice. Exaggerated ROS production in RhoA/B dKO neutrophils was further enhanced when full activation with TNF $\alpha$  and fMLF occurred (Figure 2A, third panel). This effect was independent of the priming agent (eg, LPS; data not shown) or the secondary stimulus used (C5a; supplemental Figure 2A). Inhibition of ROCK with Y-27632 did not mimic the phenotype associated with RhoA/B deficiency (supplemental Figure 2B). Phorbol ester (PMA)-stimulated ROS kinetics in WT, RhoA KO, and RhoA/B dKO neutrophils or neutrophils treated with Y-27632 were comparable, indicating that Rho is not involved in regulating the final steps of NADPH oxidase assembly or activation (Figure 2B and supplemental Figure 2B).

Attachment of neutrophils to matrix resembles migration through tissues. In these conditions, priming occurs by integrin ligation, followed by moderate but continuous ROS production upon exposure to secondary stimuli. Attached RhoA KO neutrophils released, similar to suspension neutrophils, elevated ROS upon fMLF stimulation (Figure 2C). An approximately 100% increase in H<sub>2</sub>O<sub>2</sub> release was observed in RhoA/B dKO vs WT<sup>1</sup> or RhoB KO<sup>2</sup> neutrophils. Chemoattractants and adhesion trigger the intracellular calcium flux required for neutrophil signaling and ROS generation. No alteration of stimulus-dependent temporal elevation of the cytosolic-free calcium was observed (data not shown).

### Premature NADPH oxidase assembly in RhoA/B KO neutrophils

The enhanced superoxide production in Rho-deficient neutrophils suggests altered recruitment and phosphorylation of NADPH oxidase components. Immunoblots revealed augmented translocation of the Nox2-p22<sup>phox</sup> complex, the phagocyte oxidase component p47<sup>phox</sup>, and atypical protein kinase C $\zeta$  (PKC $\zeta$ ) to the plasma membrane of RhoA/B dKO neutrophils (Figure 2D-E). Phosphorylation-dependent p47<sup>phox</sup> translocation can be mediated by PKC $\zeta$ , which targets Ser303/304 and Ser315 in fMLF-stimulated human neutrophils.<sup>30</sup> In murine WT neutrophils, the corresponding Ser316 in p47<sup>phox</sup> was transiently phosphorylated by combined TNF $\alpha$ /fMLF stimulation, whereas Ser329 phosphorylation (Ser328 human p47<sup>phox</sup>) was sustained (Figure 2F). In RhoA/B dKO neutrophils, fMLF

stimulation triggered p47<sup>phox</sup> Ser316 phosphorylation, which was further enhanced by prior TNF $\alpha$  priming (Figure 2G). TNF $\alpha$  priming by itself did not lead to Ser316 or Ser329 phosphorylation (Figure 2H). PMA-induced p47<sup>phox</sup> phosphorylation was not altered (Figure 2H), again indicating that only receptor-mediated oxidase assembly was altered by RhoA/B deficiency. MAPK are required for phosphorylation of additional sites on p47<sup>phox</sup> and p67<sup>phox</sup> proteins,<sup>4</sup> and because both p38 and Erk signaling was markedly enhanced in RhoA/B dKO neutrophils (Figure 1G and Figure 2I), it seems likely that additional phosphorylations on oxidase components occur. Premature Erk activation was solely dependent on RhoA deficiency (supplemental Figure 2C).

### Rho activity restricts the Rap/ $\beta_2$ -integrin activation complex

Integrins are essential for neutrophil adhesion and directed migration. In RhoA/B dKO neutrophils, augmented cell-surface expression of the integrin  $\beta_2$  subunit (CD18),  $\alpha_M$  subunit (CD11b), and the integrin-connected adhesion molecule CEACAM-1 was observed (Figure 3A). The cell surface expression of integrin subunits  $\beta_1$  (CD29) or  $\alpha_L$  (CD11a) was not altered, presumably because both of these molecules are not stored in granules. Binding of the  $\alpha_L\beta_2$  (LFA-1) ligand ICAM1 was elevated in RhoA/B dKO neutrophils, suggesting increased  $\beta_2$ -integrin activation (Figure 3B). ICAM1 ligand binding affinity is controlled by inside-out signaling, and in particular by formation of an integrin activation complex that relies on the GTPase Rap.<sup>31</sup> Attachment-dependent Rap1 activation was conserved in all neutrophil genotypes, whereas RhoA/B deficiency triggered premature Rap activation (Rap-GTP) in suspension neutrophils (Figure 3C). Translocation of the Rap effector RIAM<sup>32</sup> was markedly enhanced in unstimulated and fMLF-stimulated RhoA/B dKO neutrophils (Figure 3D). The reduced expression of the neutrophil semaphorin 7A receptor Plexin-C1, a Rap GTPase-activating protein,<sup>33</sup> may be involved in sustained Rap activation (Figure 3E). In addition, cooperation between the Rap-RIAM module and activated p38 (Figure 1G), a key player in  $\alpha_M\beta_2$  (Mac-1) activation,<sup>34</sup> likely triggers the increased  $\beta_2$  integrin activation observed in RhoA/B dKO neutrophils.

Increased integrin affinity often correlates with enhanced adhesion. RhoA/B dKO neutrophils and neutrophils treated with the cell-permeable RhoA-C inhibitor Tat-C3 exhibited significantly increased adhesion on fibronectin (Figure 3F-G). Prolonged adhesion/de-adhesion cycles in migrating neutrophils cause the appearance of trailing uropods. Although a transient appearance of elongated uropods was apparent in RhoA/B dKO neutrophils (Figure 3H), their overall unstimulated phenotype was surprisingly characterized by increased leading edge formation and enhanced random migration (Figure 3I, supplemental Figure 1, and supplemental Video 1).

### Rho acts as a positive and negative regulator of chemotaxis

RhoA is considered the predominant force of the “backness” program, enabling contraction and forward movement of cells. As expected, preincubation of neutrophils with Tat-C3 reduced fMLF-mediated chemotaxis of WT<sup>1</sup> neutrophils by 80% to 90% (Figure 4A). Directed migration of RhoA KO or RhoB KO neutrophils to fMLF was comparable with WT cells. In contrast, chemotaxis of RhoA/B dKO neutrophils toward fMLF was reduced by 50% (Figure 4A), indicating that the presence of either Rho isoform is sufficient for maintaining migration. Tat-C3 treatment of WT<sup>1</sup> or RhoB KO neutrophils had no effect on CXCL1-directed chemotaxis, whereas RhoA/B dKO neutrophils displayed accelerated migration (up to fourfold) toward CXCL1 (Figure 4B). The disparity between Tat-C3-mediated Rho inactivation and genetic Rho deletion phenotypes is most likely

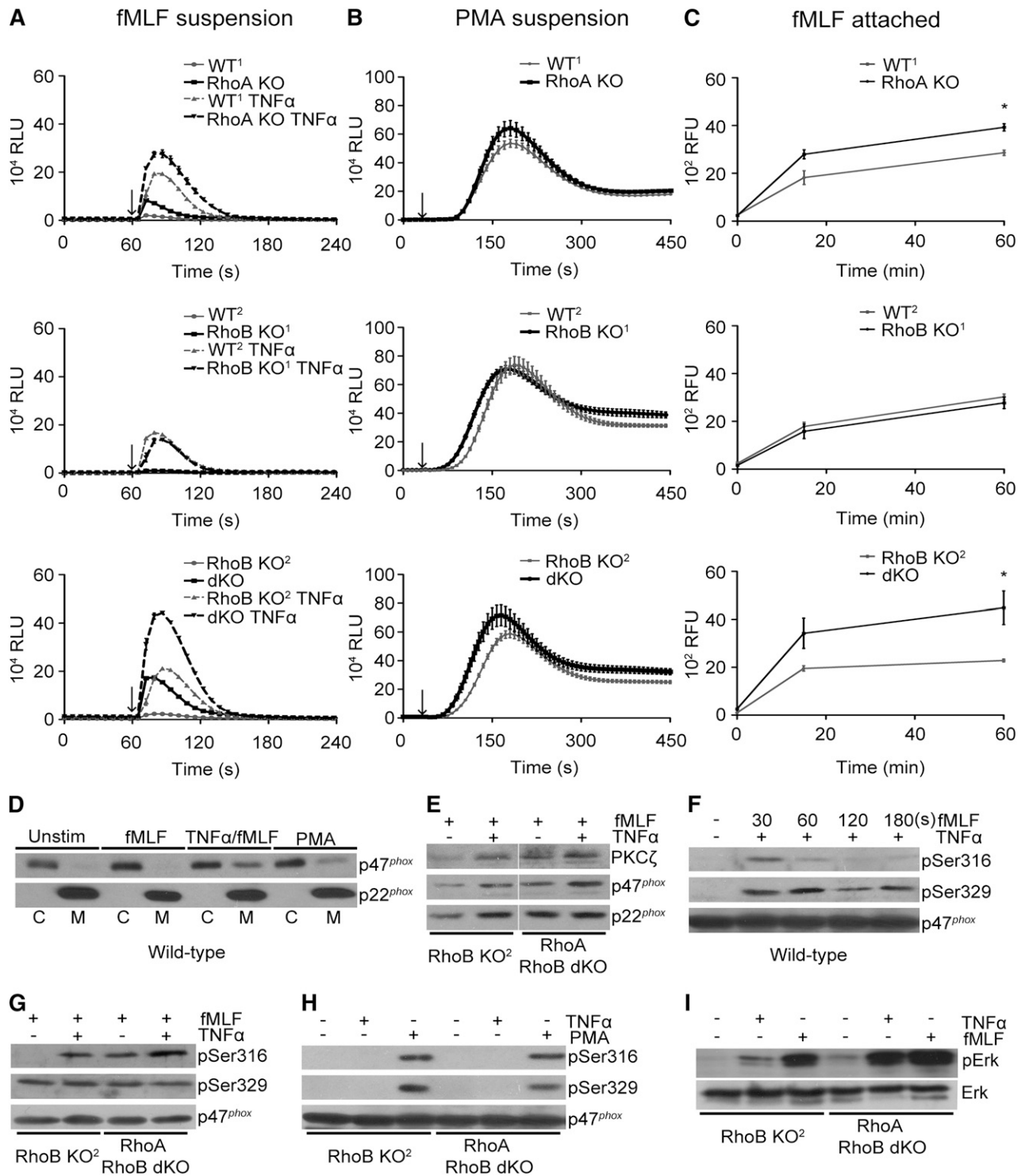


**Figure 2. RhoA acts as a negative regulator of the FPR-mediated oxidative burst.** (A-B) Superoxide production by suspension neutrophils stimulated with (A) 10  $\mu$ M fMLF with and without TNF $\alpha$  priming (10 ng/mL) or with (B) 100 ng/mL phorbol 12-myristate 13-acetate (PMA). Arrows indicate the addition of stimulus; dark black lines indicate KO responses. (C) H<sub>2</sub>O<sub>2</sub> production by adherent, fMLF-stimulated neutrophils. Stimulation at t = 0. Dark black lines indicate KO responses. (D) Immunoblot of p47<sup>phox</sup> and p22<sup>phox</sup> in cytosolic (C) and membrane (M) fractions derived from WT<sup>2</sup> neutrophils stimulated with fMLF for 5 minutes and 10 ng/mL TNF $\alpha$  for 30 minutes, followed by fMLF for 5 minutes, or with PMA for 10 minutes. (E) Immunoblot of p47<sup>phox</sup>, p22<sup>phox</sup>, and PKC $\zeta$  in membrane fractions derived from TNF $\alpha$ -primed or nonprimed RhoB KO<sup>2</sup> or RhoA/B dKO neutrophils stimulated with fMLF for 5 minutes. (F) Time course of p47<sup>phox</sup> phosphorylation during fMLF stimulation of TNF $\alpha$ -primed WT<sup>1</sup> neutrophils. (G) Comparison of fMLF-induced (30s) p47<sup>phox</sup> phosphorylation in RhoB KO<sup>2</sup> or RhoA/B dKO neutrophils in the presence or absence of TNF $\alpha$  priming. (H) Characterization of p47<sup>phox</sup> Ser316 and Ser329 phosphorylation in WT<sup>1</sup> neutrophils after stimulation with 10 ng/mL TNF $\alpha$  or 100 ng/mL PMA. (I) Erk1/2 phosphorylation in Rho-deficient suspension neutrophils stimulated with TNF $\alpha$  or fMLF as indicated; total Erk served as control. Means  $\pm$  SEM (n = 3): (C) \*P < .05, \*\*P < .01; unpaired 2-tailed Student t test.

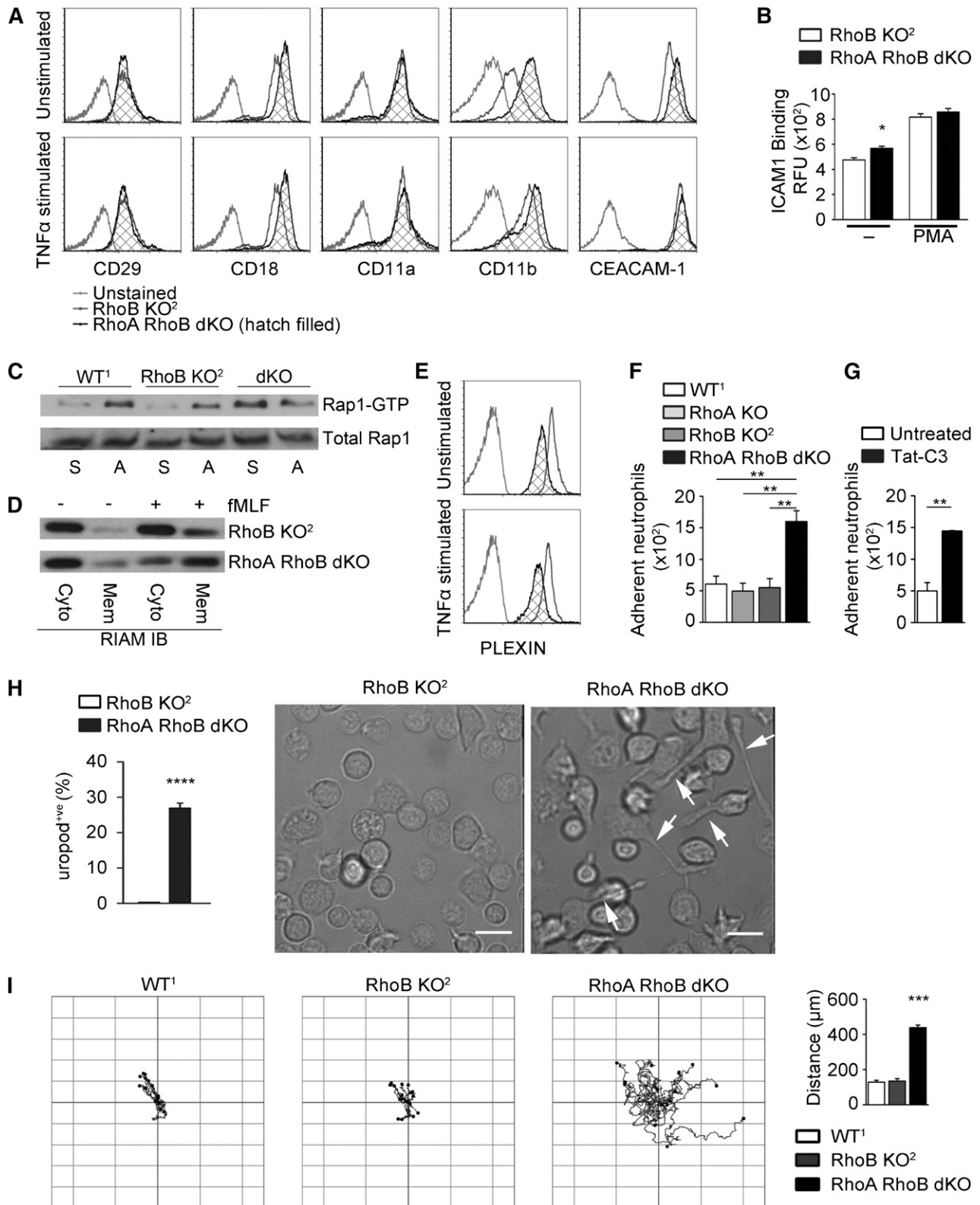


**Figure 3. Integrin/Rap-dependent proadhesive phenotype and enhanced random migration in Rho-deficient neutrophils.** (A) Cell surface expression of CD29, CD18, CD11a, CD11b, and CEACAM-1 on RhoB KO<sup>2</sup> and RhoA/B dKO neutrophils. (B) Flow cytometry analysis of ICAM1/Fc binding to unstimulated or PMA-stimulated RhoB KO<sup>2</sup> and RhoA/B dKO neutrophils. (C) Rap GTPase activation in WT<sup>1</sup>, RhoB KO<sup>2</sup>, and RhoA/B dKO neutrophils in suspension (S) or adhered to fibronectin (A). Total Rap served as control. (D) RIAM translocation analyzed in membrane (Mem) and cytosol (Cyto) fractions derived from unstimulated or fMLF-stimulated RhoB KO<sup>2</sup> or RhoA/B dKO neutrophils. (E) Cell surface expression of Plexin-B1 in RhoB KO<sup>2</sup> and RhoA/B dKO neutrophils. (F-G) Static adhesion assay comparing (F) neutrophils of indicated genotypes and (G) WT neutrophils with and without Tat-C3 pretreatment. (H) Quantification of uropod retraction defects during haptotaxis expressed as percentage of neutrophils displaying trailing uropods ( $n = 4$ ; images represent 4 independent fields per experiment). The scale bar represents 10  $\mu$ m. (I) Neutrophil tracking during random migration (left,  $n = 3$ ), quantification of total distance migrated per neutrophil (right,  $***P < .005$  by 1-way ANOVA post hoc Dunnett's multiple variance test). Means  $\pm$  SEM ( $n = 3$ ): (B,F,G,H)  $*P < .05$ ,  $**P < .01$ ,  $***P < .005$ ,  $****P < .0001$  by unpaired 2-tailed Student  $t$  test.

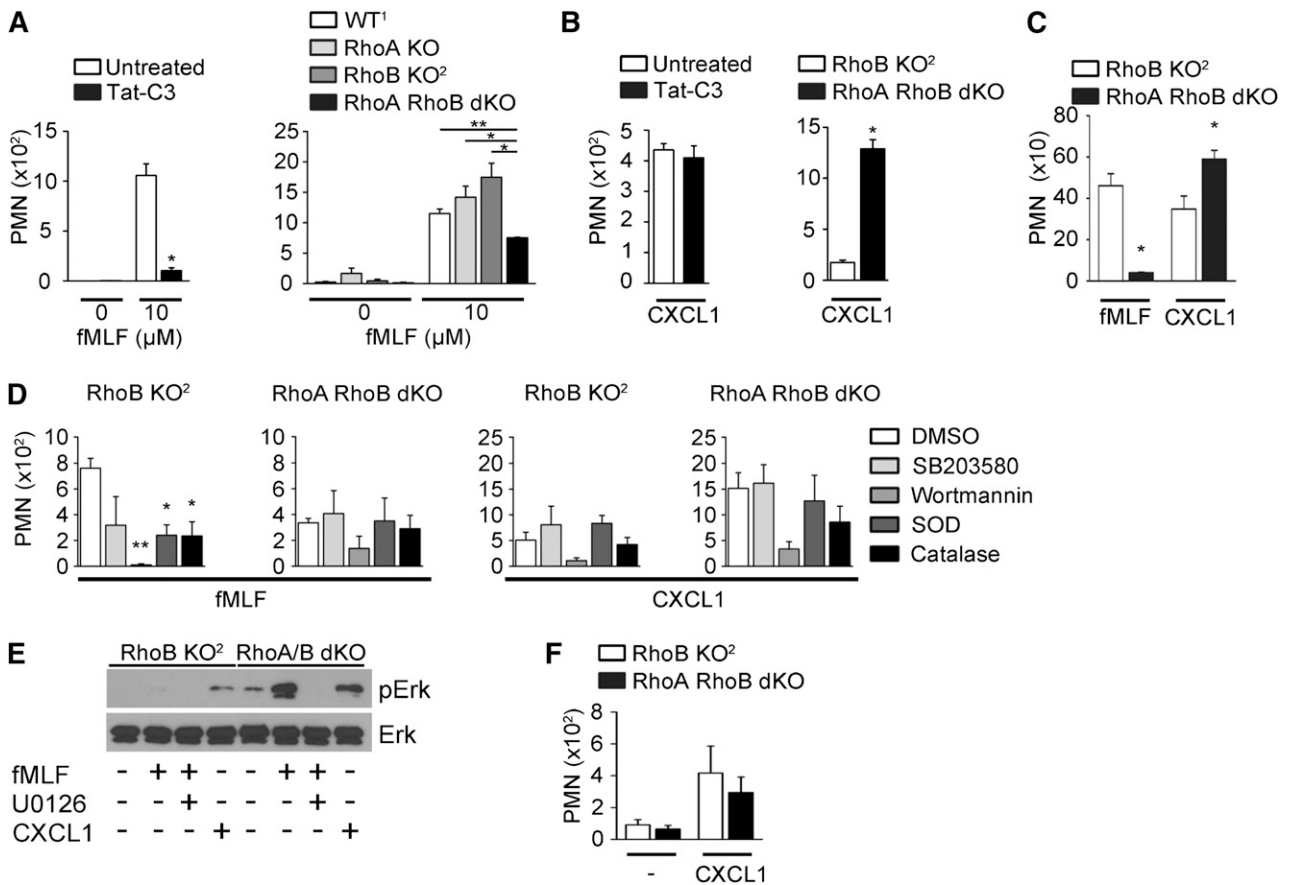


**Figure 4. In vitro migration of Rho-deficient neutrophils is stimulus dependent.** (A) Migration of WT neutrophils through Boyden chambers toward fMLF with or without Tat-C3 pretreatment (left panel) or of the indicated genotypes (right panel). (B) Migration of WT neutrophils through Boyden chambers toward CXCL1 with or without Tat-C3 pretreatment (left panel) or of the indicated genotypes (right panel). (C) Migration of neutrophils toward fMLF or CXCL1 through type 1 collagen. (D) Migration of RhoB KO<sup>2</sup> or RhoA/B dKO neutrophils toward either fMLF or CXCL1 after inhibitor pretreatment. (E) Immunoblot depicting Erk (p42/44 MAPK) phosphorylation in attached Rho-deficient neutrophils stimulated with fMLF (+/- 5 µM U0126) or CXCL1; total Erk served as the loading control. (F) Migration of neutrophils toward CXCL1 through 5-µm pore filters. Means ± SEM (n = 3): (A-C) \*P < .05, \*\*P < .01 by unpaired 2-tailed Student *t* test; (D) \*P < .05, \*\*P < .01, by 1-way ANOVA post hoc Dunnett's multiple variance test.

caused by an inefficiency of short-term Tat-C3 treatment and/or more generalized changes elicited by Rho deficiency. To mimic movement in interstitial tissue, neutrophil chemotaxis through fibrillar collagen I was analyzed.<sup>35</sup> In RhoA/B dKO neutrophils, migration toward fMLF was again markedly decreased, whereas CXCL1-induced chemotaxis was augmented (Figure 4C).

Neutrophil migration to different cues is mediated by the dynamic localization of the phosphatidylinositol 3-kinase (PI3K) product PI(3,4,5)P<sub>3</sub> and by p38 and Erk activation. Although PI3K activity is essential for fMLF- and CXCL1-induced migration, p38 signaling is only involved in fMLF-directed chemotaxis.<sup>36</sup> RhoB KO neutrophils responded accordingly to inhibitors of PI3K (wortmannin) and p38 (SB203580), whereas p38 signaling in RhoA/B dKO neutrophils seems to be refractory to pharmacologic inhibition (Figure 4D). MEK1/2-Erk signaling, a prerequisite for fMLF- and CXCL1-induced motility (supplemental Figure 3A), was highly upregulated in adherent, fMLF-stimulated RhoA/B dKO neutrophils (Figure 4E). End-target chemoattractants (fMLF, C5a), but not intermediary chemoattractants (CXCL1), trigger NADPH oxidase activation and ROS production in attached neutrophils. To test whether H<sub>2</sub>O<sub>2</sub> feedback signaling, which will inactivate phosphatases,<sup>37</sup> affects neutrophil migration, SOD and catalase were added during chemotaxis. Both treatments decreased fMLF-induced chemotaxis in RhoB KO neutrophils but had no effect on RhoA/B dKO neutrophils or on CXCL1-induced chemotaxis (Figure 4D). Similarly, inhibition of

Nox2 activity with diphenylene iodonium did not alter chemotaxis of RhoA/B dKO neutrophils (supplemental Figure 3B). Alternatively, enhanced chemotaxis of RhoA/B dKO neutrophils toward CXCL1 could be caused by enhanced deformability. Indeed, comparable migration of RhoB KO and RhoA/B dKO neutrophils was observed when the filter pore size was increased (Figure 4F). Taken together, Rho limits MAPK activity and regulates cytoskeletal shape changes. Both are part of efficient chemotaxis toward end targets but seem dispensable for migration toward intermediary chemoattractants.

**Rho deletion promotes chemotaxis in vivo**

Commonly, Rho activity has been considered essential for cell migration. Because CXCL1 and its receptor CXCR2 mediate neutrophil chemotaxis in response to many cues, the unexpected increase in CXCL1-mediated migration by RhoA/B dKO neutrophils suggested that in contrast to the prevailing notion, Rho activity may suppress neutrophil migration in vivo. Rapid neutrophil influx into the peritoneum permits quantitative analysis of neutrophil migration. In sterile inflammation induced by thioglycollate, the number of emigrated neutrophils increased up to fourfold in RhoA/B dKO mice compared with RhoB KO<sup>2</sup> mice (Figure 5A and supplemental Figure 4A). Neutrophil influx in RhoA KO mice was only slightly augmented, again highlighting that RhoB upregulation can compensate for RhoA deficiency, whereas the phenotype of

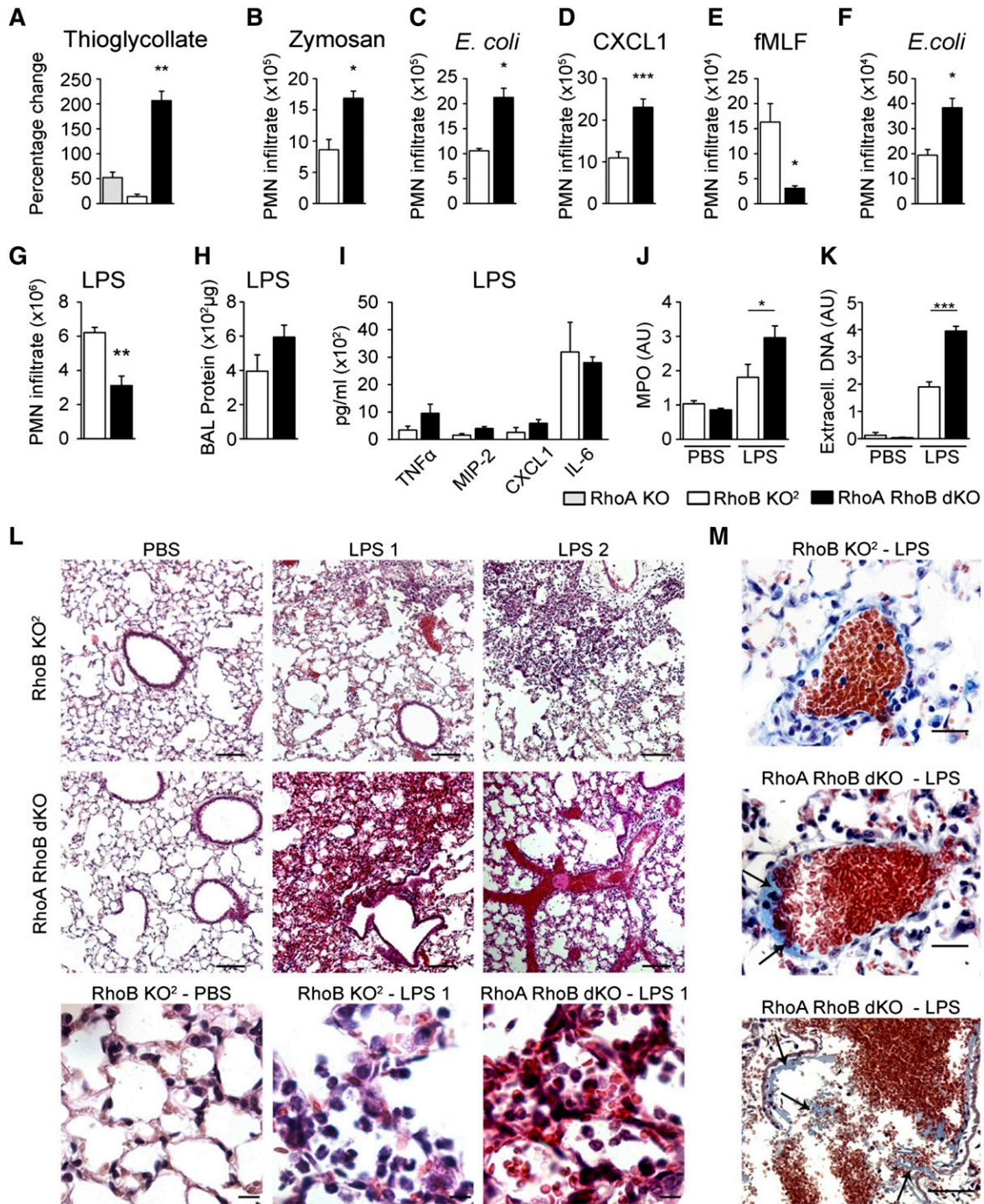


**Figure 5. Rho deficiency alters in vivo neutrophil emigration and augments LPS-induced ALI.** (A) Influx of neutrophils in RhoA KO, RhoB KO<sup>2</sup>, or RhoA/B dKO mice 5 hours after ip thioglycollate injection (n = 5). (B-C) Peritoneal neutrophil infiltrate in RhoB KO<sup>2</sup> or RhoA/B dKO mice 5 hours after ip injection with (B) zymosan (n = 3) and (C) *E. coli* (n = 8). (A) Data are presented as percentage change in peritoneal neutrophils (% migration) of RhoA KO, RhoB KO<sup>1</sup>, and RhoA/B dKO mice compared with their controls WT<sup>1</sup>, WT<sup>2</sup>, and RhoB KO<sup>2</sup>, respectively. (D-G) Quantification of neutrophils in lung BAL fluid 5 hours after in challenge with (D) CXCL1 (n = 4), (E) fMLF (n = 4), or (F) *E. coli* (n = 3), or 24 hours after (G) LPS (n = 7). (H-K) Protein (H) (n = 4), chemokine and cytokine (I) (n = 4) content, MPO activity (J) (n = 4), and NET formation (K) (n = 3) within BAL collected from RhoB KO<sup>2</sup> or RhoA/B dKO mice 24 hours after in challenge with LPS. AU, arbitrary units. (L) Hematoxylin and eosin staining of lung tissue 24 hours after LPS instillation; the scale bar represents 200  $\mu$ m (images 1-6) and 20  $\mu$ m (images 7-9). Images are representative of 20 fields per section, 3 sections per lung, 4 lungs per genotype per experiment. (M) Modified Carstairs staining performed on lung tissue as in (L); the scale bar represents 1  $\mu$ m (upper 2 panels) and 200  $\mu$ m (lower panel). Images are representative of 30 fields per section, 2 sections per lung, 3 lungs per genotype per experiment. (A-K) Data are pooled from 3 experiments. Means  $\pm$  SEM (n indicated): (A-J) \**P* < .05, \*\**P* < .01, \*\*\**P* < .005 by unpaired 2-tailed Student *t* test.

RhoB KO<sup>1</sup> mice resembled WT<sup>2</sup> mice. To analyze chemoattractant-induced in vivo migration, pathogen-based models of inflammatory peritonitis were used. Injection of *Saccharomyces cerevisiae* particles (zymosan) significantly augmented neutrophil influx in RhoA/B

dKO mice (Figure 5B). Similarly, injection of *E. coli* into the peritoneum of RhoA RhoB dKO mice replicated the gain in neutrophil transmigration (Figure 5C). Comparison of peritoneal neutrophils derived from RhoB KO and RhoA/B dKO mice after



thioglycollate injection revealed that although appearance and attachment of neutrophils was now comparable, fMLF-stimulated ROS production was still elevated (supplemental Figure 4B-E).

### Rho deficiency leads to stimulus-specific neutrophil influx into the lung

Neutrophil sequestration in pulmonary capillaries and emigration into the lungs are less dependent on adhesion and matrix degradation than neutrophil emigration from the systemic circulation. Further, the pathways required for neutrophil emigration in response to particular stimuli differ and are classified as either  $\beta_2$  integrin-dependent or -independent. Although fMLF is considered  $\beta_2$  integrin-dependent, CXCL1 acts independently of  $\beta_2$  integrins.<sup>38</sup> Neutrophil emigration by intranasal challenge with fMLF or CXCL1 could thus serve as an in vivo model to validate the functionally opposing roles of Rho observed in vitro. In fact, neutrophil flux after exposure to both stimuli mirrored the in vitro chemotaxis results. RhoA/B dKO neutrophils migrated significantly faster into the lungs upon CXCL1 challenge, whereas migration toward fMLF was strongly inhibited (Figure 5D-E). Intranasal infection with *E coli* recruited neutrophils rapidly into the airways, leading similar to peritoneal challenge, to significantly increased neutrophil influx in RhoA/B dKO mice (Figure 5F). Migration upon LPS challenge is considered  $\beta_2$  integrin-dependent and serves as a model for ALI. Similar to the fMLF challenge, LPS-induced neutrophil recruitment was inhibited in RhoA/B dKO mice (Figure 5G). Because of the extended time course of LPS-mediated lung injury, Rho deficiency in alveolar macrophages could contribute to the phenotype. LPS-stimulated macrophages of all genotypes showed comparable cytokine/chemokine profiles and Cox-2 upregulation (supplemental Figure 5A). The reduced neutrophil influx in LPS-challenged RhoA/B dKO mice did not lead to significant attenuation of lung injury parameters such as BAL protein content, wet-to-dry lung:weight ratio (not shown), or cytokine/chemokine release (Figure 5H-I), but increased MPO activity and NET formation (Figure 5J-K), most likely as a result of the hyperresponsiveness of RhoA/B dKO neutrophils. Myeloid RhoA/B deficiency amplified pulmonary tissue injury, causing hemorrhage, platelet recruitment, and clot formation (Figure 5L-M).

### Absence of Rho rescues from lethal IAV infection

In contrast to ALI, resolution of IAV-induced pneumonia relies on an efficient influx of highly activated neutrophils.<sup>39</sup> RhoA/B dKO neutrophils possess a hyperresponsive phenotype that may be beneficial in viral infections. The clinical isolate of pandemic 2009H1N1 IAV shows host-specific pathogenicity in mice.<sup>40</sup> Intranasal IAV infection caused exaggerated neutrophil influx into the lungs of RhoA/B dKO mice within 24 hours, which was fivefold higher than the influx in RhoB KO<sup>2</sup> mice (Figure 6A). These neutrophils were highly activated, leading to increased BAL protein content and MPO release (Figure 6B-C). Two days later, neutrophil counts were still twofold elevated in RhoA/B dKO mice (Figure 6D). Chemokine, cytokine, and type I interferon levels in BAL fluid were moderately augmented (Figure 6E-F). The increase in soluble mediators may be partially caused by virus-triggered alveolar macrophage responses because poly-IC-stimulated RhoA/B dKO macrophages released higher levels of chemokines and cytokines (supplemental Figure 5B). Neutrophils recovered from lungs 72 hours after IAV challenge showed enhanced CRAMP expression (Figure 6G) and a 200% increase of intracellular viral matrix protein 1 (M1) (Figure 6H). Although IAV titers did not correlate with disease outcome in WT mice,<sup>24</sup> a significant

reduction in virus load was detected in lung tissue obtained from RhoA/B dKO mice (Figure 6I). The time course of IAV infection was then extended to 7 days. Body weight dropped between days 2 and 3 in WT<sup>1</sup>, RhoB KO<sup>2</sup>, and RhoA/B dKO mice. However, although RhoA/B dKO mice never lost >10% body weight, WT<sup>1</sup> and RhoB KO<sup>2</sup> mice continued to not only lose body weight but they also displayed severe respiratory distress and general malaise that required euthanasia between days 3 and 4 (Figure 6J-K). RhoA/B dKO mice showed only intermittent mild disease symptoms and all of the mice survived IAV challenge until day 7, when the experiment was terminated.

### Discussion

Targeting neutrophil recruitment to inflammatory sites and their activation state is a principal goal for the development of anti-inflammatory therapies. This study shows the intricate connections between neutrophil responses that lead to unexpected outcomes. Signaling pathways under the control of cytoskeletal regulators such as Rho GTPases affect several fundamental processes in a manner that cannot always be deduced from inhibitor studies or other cell types. A case in point is this study, where RhoA maintains neutrophil quiescence, controls priming responses, and discriminates between chemotactic stimuli, acting as negative regulator of  $\beta_2$ -independent neutrophil motility. Neutrophil RhoB is expendable, although it can compensate for RhoA to some extent. RhoB was markedly upregulated in RhoA-deficient neutrophils, most likely because of posttranscriptional stabilization.<sup>41</sup> Although RhoA deficiency triggered granule exocytosis and elevated ROS generation even in the presence of RhoB upregulation, the phenotype of RhoA/B dKO neutrophils was consistently more severe. Generalized preactivation in Rho-deficient neutrophils led to a complex phenotype. As many as 250 proteins including receptors, integrins, the Nox2-p22<sup>phox</sup> oxidase complex, GTPases, proteases, antimicrobial peptides, and alarmins will be released upon granule exocytosis.<sup>42</sup> Functionally, priming is best characterized as a prerequisite for an efficient oxidative burst.<sup>4</sup> RhoA/B dKO neutrophils generated exaggerated levels of superoxide, which can be beneficial or detrimental depending on the disease context.

Activated integrin signaling constitutes another priming response. Formation of the active Rap1-GTP/RIAM module, as observed upon Rho deletion, mediates integrin activation by RIAM-induced talin recruitment,<sup>31</sup> leading to increased ICAM1 binding and adhesion. Constitutive Rap1 activity may ensue from CalDAG-GEFI and p38 MAPK signaling,<sup>43</sup> because CalDAG-GEFI-deficient neutrophils showed  $\beta_2$  integrin-dependent loss of adhesion and/or from defects in Rap1 GDP hydrolysis. In addition, Rap1 activity can also trigger signaling via Radil or RAPL and may increase Arf6 inactivation by stimulating the GAP ARAP3.<sup>44</sup> Although strengthening of adhesive signaling usually triggers decreased motility, RhoA/B dKO neutrophils were highly motile without stimulation.

Directed migration was also increased upon almost all challenges. These observations are not in line with the current paradigm that RhoA is essential for front protrusion and back retraction of migrating cells.<sup>45</sup> Neutrophil migration in response to CXCL1, thioglycollate, zymosan particles, *E coli*, and IAV was strikingly augmented in the absence of Rho proteins, clearly indicating that Rho acts primarily as a negative regulator of migration in vivo. Common to all stimuli, usually restricted by Rho activity, is their  $\beta_2$  integrin independence when triggering neutrophil influx.<sup>38,46</sup>  $\beta_2$ -integrin involvement in *E coli*-mediated chemotaxis has been controversial, but more recent studies by Ong and coworkers<sup>47</sup> support our hypothesis that RhoA controls  $\beta_2$ -dependent and -independent pathways, albeit in a positive or negative manner. Reducing the need for cytoskeletal deformation

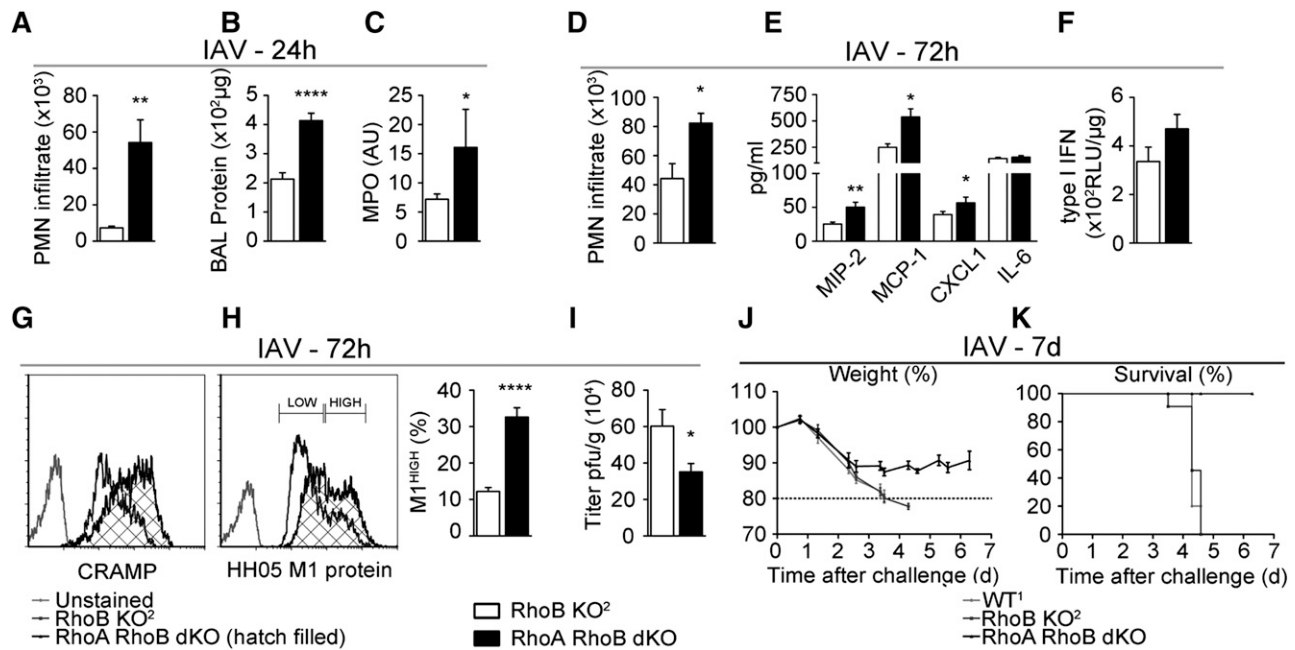


**Figure 6. Rho deficiency in innate immune cells protects against IAV infection.** (A-C) Neutrophil load (A), protein content (B), and MPO activity (C) in BAL fluid of RhoB KO<sup>2</sup> or RhoA/B dKO mice 24 hours after instillation of IAV pHH05 ( $1 \times 10^6$  PFU/kg). (D-F) Neutrophil load (D), chemokine and cytokine release (E), and type I interferon content (F) in the BAL fluid of RhoB KO<sup>2</sup> or RhoA/B dKO mice 72 hours after IAV challenge. (G) CRAMP surface expression on BAL fluid neutrophils derived from RhoB KO<sup>2</sup> or RhoA/B dKO mice (72 hours). (H) Virus uptake by neutrophils detected as matrix protein M1 (left, flow cytometry histogram; right, quantification) (72 hours). (I) Virus titer in lung tissue 72 hours after IAV infection. (A-I) Data are pooled from 3 experiments. Means  $\pm$  SEM: (A-C,  $n = 5$ ), (D-I,  $n = 7$ ). (A-F, H [right]-I)  $*P < .05$ ,  $**P < .01$ ,  $***P < .001$ ,  $****P < .0001$  by unpaired 2-tailed Student *t* test. (J-K) Weight loss (J) and survival curve (K) of WT<sup>1</sup>, RhoB KO<sup>2</sup>, and RhoA/B dKO mice during IAV infection (7 days) ( $n = 8$  per group). Mann-Whitney *U* rank-sum test for weight loss at 84 hours: RhoB vs RhoA/B,  $P < .0005$ ; Gehan-Breslow-Wilcoxon test for Kaplan-Meier survival analysis WT<sup>1</sup> vs RhoA/B,  $P < .0005$ ; RhoB vs RhoA/B,  $P < .005$ ; WT<sup>1</sup> vs RhoB,  $P = .5421$ .

offset the gain in CXCL1-directed migration, suggesting that RhoA is not essential for gradient sensing but controls structural changes required for deformation. Transmigrating WT neutrophils execute rapid but transient cytoskeletal changes such as F-actin rims.<sup>48,49</sup> This neutrophil deformability is spatiotemporally fine-tuned, permitting deformation when passing through pulmonary capillaries, followed by cell stiffening for sequestration. This scenario is difficult to address experimentally because increasing the pore size also reduces the steepness of the chemotactic gradient, which affects velocity by altering concentration and/or localization of PI(3,4,5)P<sub>3</sub>, lipid mediators, adenosine triphosphate, and alarmins. Moreover, RhoA may restrict integrin-independent actin flow *in vivo*,<sup>50</sup> and further studies will be required to clarify this point.

Therapeutically targeting Rho signaling in innate immune cells has been proposed for ALI. The results of this study suggest that at least in terms of LPS-induced lung damage, this approach will not lead to amelioration of the inflammatory phenotype, even though neutrophil numbers in the lung were substantially reduced. In fact, hyperactivation of RhoA/B dKO neutrophils was critical in propagating injury, possibly by enhanced binding to the endothelial wall and tissue factor activation, initiating platelet accumulation and thrombus formation.<sup>51</sup> Thus novel strategies for preventing neutrophil-associated lung injury may need to focus primarily on restricting degranulation. In contrast, features such as nonproductive virus uptake, NET formation, and regulation of dendritic cells and T cells place neutrophils as desirable first responders in viral infections. Endocytosis of viral particles was more efficient in BAL neutrophils derived from IAV-challenged RhoA/B dKO mice, although uptake of fluorescent dextran was comparable in RhoB KO and RhoA/B dKO neutrophils *in vitro* (data not shown). The prolonged time course of IAV infection will trigger responses from other immune cells, but the immediate influx of activated neutrophils releasing MPO

and CRAMP and their increased virus uptake was likely responsible for survival of RhoA/B dKO mice. Importantly, although neutrophils cannot generate infectious viral particles, they can serve as antigen-presenting cells for antiviral CD8<sup>+</sup> T cells.<sup>52</sup> Because increased influx of activated neutrophils will be highly desirable in IAV or respiratory syncytial virus infections, a direct drug-targeting approach for Rho proteins could be beneficial for resolution of viral lung diseases.

## Acknowledgments

The authors thank G. Prendergast and G. Gabriel for critical reagents; and M. Murphy, P. Hanley, M. Tsatmali, and B. Bourke for assistance and discussions.

This work was supported by funding from the Health Research Board and Science Foundation Ireland (U.G.K.); by INSERM, Centre National de la Recherche Scientifique, and Inflammex (J.E.B.); and by the Danish Research Foundation (C.B.). U.G.K. is the recipient of an Science Foundation Ireland Stokes award.

## Authorship

Contribution: R.T.J. and U.G.K. designed experiments, analyzed data, and wrote the paper; R.T.J. performed the majority of the experiments; M.S., M.K., and P.H. performed experiments and analyzed data; J.E.-B. developed p47<sup>phox</sup> antibodies; and C.B. generated the RhoA<sup>ff</sup> mice.

Conflict-of-interest disclosure: The authors declare no competing financial interests.

Correspondence: Ulla Knaus, Conway Institute, University College Dublin, Belfield, Dublin 4, Ireland; e-mail: ulla.knaus@ucd.ie.

## References

- Sadik CD, Kim ND, Luster AD. Neutrophils cascading their way to inflammation. *Trends Immunol.* 2011;32(10):452-460.
- Mocsai A. Diverse novel functions of neutrophils in immunity, inflammation, and beyond. *J Exp Med.* 2013;210(7):1283-1299.
- Kolaczowska E, Kubes P. Neutrophil recruitment and function in health and inflammation. *Nat Rev Immunol.* 2013;13(3):159-175.
- El-Benna J, Dang PM, Gougerot-Pocidalo MA. Priming of the neutrophil NADPH oxidase activation: role of p47phox phosphorylation and NOX2 mobilization to the plasma membrane. *Semin Immunopathol.* 2008;30(3):279-289.
- Sit ST, Manser E. Rho GTPases and their role in organizing the actin cytoskeleton. *J Cell Sci.* 2011; 124(Pt 5):679-683.
- Heasman SJ, Ridley AJ. Mammalian Rho GTPases: new insights into their functions from in vivo studies. *Nat Rev Mol Cell Biol.* 2008;9(9): 690-701.
- Pedersen E, Brakebusch C. Rho GTPase function in development: how in vivo models change our view. *Exp Cell Res.* 2012;318(14):1779-1787.
- Mulloy JC, Cancelas JA, Filipi MD, Kalfa TA, Guo F, Zheng Y. Rho GTPases in hematopoiesis and hemopathies. *Blood.* 2010;115(5):936-947.
- Abdel-Latif D, Steward M, Lacy P. Neutrophil primary granule release and maximal superoxide generation depend on Rac2 in a common signalling pathway. *Can J Physiol Pharmacol.* 2005;83(1):69-75.
- Thumkeo D, Watanabe S, Narumiya S. Physiological roles of Rho and Rho effectors in mammals. *Eur J Cell Biol.* 2013;92(10-11): 303-315.
- Heasman SJ, Carlin LM, Cox S, Ng T, Ridley AJ. Coordinated RhoA signaling at the leading edge and uropod is required for T cell transendothelial migration. *J Cell Biol.* 2010;190(4):553-563.
- Cavnar PJ, Berthier E, Beebe DJ, Huttenlocher A. Hax1 regulates neutrophil adhesion and motility through RhoA. *J Cell Biol.* 2011;193(3):465-473.
- Caron E, Hall A. Identification of two distinct mechanisms of phagocytosis controlled by different Rho GTPases. *Science.* 1998; 282(5394):1717-1721.
- Colucci-Guyon E, Niedergang F, Wallar BJ, Peng J, Alberts AS, Chavrier P. A role for mammalian diaphanous-related formins in complement receptor (CR3)-mediated phagocytosis in macrophages. *Curr Biol.* 2005;15(22):2007-2012.
- Hall AB, Gakidis MA, Glogauer M, et al. Requirements for Vav guanine nucleotide exchange factors and Rho GTPases in FcγR-mediated and complement-mediated phagocytosis. *Immunity.* 2006;24(3):305-316.
- Jackson B, Peyrollier K, Pedersen E, et al. RhoA is dispensable for skin development, but crucial for contraction and directed migration of keratinocytes. *Mol Biol Cell.* 2011;22(5):593-605.
- Clausen BE, Burkhardt C, Reith W, Renkawitz R, Förster I. Conditional gene targeting in macrophages and granulocytes using LysMcre mice. *Transgenic Res.* 1999;8(4):265-277.
- Liu AX, Rane N, Liu JP, Prendergast GC. RhoB is dispensable for mouse development, but it modifies susceptibility to tumor formation as well as cell adhesion and growth factor signaling in transformed cells. *Mol Cell Biol.* 2001;21(20): 6906-6912.
- Siemsen DW, Schepetkin IA, Kirpotina LN, Lei B, Quinn MT. Neutrophil isolation from nonhuman species. *Methods Mol Biol.* 2007;412:21-34.
- Jennings RT, Knaus UG. Neutrophil migration through extracellular matrix. *Methods Mol Biol.* 2014;1124:209-218.
- Jennings RT, Knaus UG. Rho family and Rap GTPase activation assays. *Methods Mol Biol.* 2014;1124:79-88.
- Abdel-Latif D, Steward M, Macdonald DL, Francis GA, Dinauer MC, Lacy P. Rac2 is critical for neutrophil primary granule exocytosis. *Blood.* 2004;104(3):832-839.
- von Löhneysen K, Noack D, Jesaitis AJ, Dinauer MC, Knaus UG. Mutational analysis reveals distinct features of the Nox4-p22 phox complex. *J Biol Chem.* 2008;283(50):35273-35282.
- Otte A, Sauter M, Alleva L, Baumgarte S, Klingel K, Gabriel G. Differential host determinants contribute to the pathogenesis of 2009 pandemic H1N1 and human H5N1 influenza A viruses in experimental mouse models. *Am J Pathol.* 2011; 179(1):230-239.
- Manukyan M, Nalbant P, Luxen S, Hahn KM, Knaus UG. RhoA GTPase activation by TLR2 and TLR3 ligands: connecting via Src to NF-κB. *J Immunol.* 2009;182(6):3522-3529.
- Matrosovich M, Matrosovich T, Garten W, Klenk HD. New low-viscosity overlay medium for viral plaque assays. *Viral J.* 2006;3:63.
- Strengert M, Jennings R, Davanture S, Hayes P, Gabriel G, Knaus UG. Mucosal Reactive Oxygen Species Are Required for Antiviral Response: Role of Duox in Influenza A Virus Infection. *Antioxid Redox Signal.* 2013. [Epub ahead of print].
- Jog NR, Rane MJ, Lominadze G, Luerman GC, Ward RA, McLeish KR. The actin cytoskeleton regulates exocytosis of all neutrophil granule subsets. *Am J Physiol Cell Physiol.* 2007;292(5): C1690-C1700.
- Ward RA, Nakamura M, McLeish KR. Priming of the neutrophil respiratory burst involves p38 mitogen-activated protein kinase-dependent exocytosis of flavocytochrome b558-containing granules. *J Biol Chem.* 2000;275(47): 36713-36719.
- Dang PM, Fontayne A, Hakim J, El Benna J, Périain A. Protein kinase C zeta phosphorylates a subset of selective sites of the NADPH oxidase component p47phox and participates in formyl peptide-mediated neutrophil respiratory burst. *J Immunol.* 2001;166(2):1206-1213.
- Abram CL, Lowell CA. The ins and outs of leukocyte integrin signaling. *Annu Rev Immunol.* 2009;27:339-362.
- Lee HS, Lim CJ, Puzon-McLaughlin W, Shattil SJ, Ginsberg MH. RIAM activates integrins by linking talin to ras GTPase membrane-targeting sequences. *J Biol Chem.* 2009;284(8):5119-5127.
- Wang Y, He H, Srivastava N, et al. Plexins are GTPase-activating proteins for Rap and are activated by induced dimerization. *Sci Signal.* 2012;5(207):ra6.
- Detmers PA, Zhou D, Polizzi E, et al. Role of stress-activated mitogen-activated protein kinase (p38) in beta 2-integrin-dependent neutrophil adhesion and the adhesion-dependent oxidative burst. *J Immunol.* 1998;161(4):1921-1929.
- Van Goethem E, Poincloux R, Gauffre F, Maridonneau-Parini I, Le Cabec V. Matrix architecture dictates three-dimensional migration modes of human macrophages: differential involvement of proteases and podosome-like structures. *J Immunol.* 2010;184(2):1049-1061.
- Heit B, Robbins SM, Downey CM, et al. PTEN functions to 'prioritize' chemotactic cues and prevent 'distraction' in migrating neutrophils. *Nat Immunol.* 2008;9(7):743-752.
- Kuiper JW, Sun C, Magalhães MA, Glogauer M. Rac regulates PtdInsP<sub>3</sub> signaling and the chemotactic compass through a redox-mediated feedback loop. *Blood.* 2011;118(23):6164-6171.
- Mackarel AJ, Russell KJ, Brady CS, FitzGerald MX, O'Connor CM. Interleukin-8 and leukotriene-B(4), but not formylmethionyl leucylphenylalanine, stimulate CD18-independent migration of neutrophils across human pulmonary endothelial cells in vitro. *Am J Respir Cell Mol Biol.* 2000; 23(2):154-161.
- Tate MD, Deng YM, Jones JE, Anderson GP, Brooks AG, Reading PC. Neutrophils ameliorate lung injury and the development of severe disease during influenza infection. *J Immunol.* 2009; 183(11):7441-7450.
- Otte A, Gabriel G. 2009 pandemic H1N1 influenza A virus strains display differential pathogenicity in C57BL/6J but not BALB/c mice. *Virulence.* 2011; 2(6):563-566.
- Ho TT, Merajver SD, Lapière CM, Nuscgens BV, Deroanne CF. RhoA-GDP regulates RhoB protein stability. Potential involvement of RhoGDIIalpha. *J Biol Chem.* 2008;283(31):21588-21598.
- Lominadze G, Powell DW, Luerman GC, Link AJ, Ward RA, McLeish KR. Proteomic analysis of human neutrophil granules. *Mol Cell Proteomics.* 2005;4(10):1503-1521.
- Stadtmann A, Brinkhaus L, Mueller H, et al. Rap1a activation by CalDAG-GEFI and p38 MAPK is involved in E-selectin-dependent slow leukocyte rolling. *Eur J Immunol.* 2011;41(7): 2074-2085.
- Gloerich M, Bos JL. Regulating Rap small G-proteins in time and space. *Trends Cell Biol.* 2011;21(10):615-623.
- Infante E, Ridley AJ. Roles of Rho GTPases in leucocyte and leukaemia cell transendothelial migration. *Philos Trans R Soc Lond B Biol Sci.* 2013;368(1629):20130013.
- Doerschuk CM, Tasaka S, Wang Q. CD11/ CD18-dependent and -independent neutrophil emigration in the lungs: how do neutrophils know which route to take? *Am J Respir Cell Mol Biol.* 2000;23(2):133-136.
- Ong ES, Gao XP, Xu N, et al. E. coli pneumonia induces CD18-independent airway neutrophil migration in the absence of increased lung vascular permeability. *Am J Physiol Lung Cell Mol Physiol.* 2003;285(4):L879-L888.
- Worthen GS, Schwab B III, Elson EL, Downey GP. Mechanics of stimulated neutrophils: cell stiffening induces retention in capillaries. *Science.* 1989;245(4914):183-186.
- Yoshida K, Kondo R, Wang Q, Doerschuk CM. Neutrophil cytoskeletal rearrangements during capillary sequestration in bacterial pneumonia in rats. *Am J Respir Crit Care Med.* 2006;174(6): 689-698.
- Huttenlocher A, Horwitz AR. Integrins in cell migration. *Cold Spring Harb Perspect Biol.* 2011; 3(9):a005074.
- Darbousset R, Thomas GM, Mezouar S, et al. Tissue factor-positive neutrophils bind to injured endothelial wall and initiate thrombus formation. *Blood.* 2012;120(10):2133-2143.
- Aarbiou J, Copreni E, Buijs-Offerman RM, et al. Lentiviral small hairpin RNA delivery reduces apical sodium channel activity in differentiated human airway epithelial cells. *J Gene Med.* 2012; 14(12):733-745.